The Beeman Formation (Upper Pennsylvanian) of the Sacramento Mountains, New Mexico: Guide to the Dry Canyon area with discussion on shelf and basin responses to eustasy, tectonics, and climate

William D. Raatz and J. A. (Toni) Simo

1998, pp. 161-176. https://doi.org/10.56577/FFC-49.161

in:

Las Cruces Country II, Mack, G. H.; Austin, G. S.; Barker, J. M.; [eds.], New Mexico Geological Society 49 th Annual Fall Field Conference Guidebook, 325 p. https://doi.org/10.56577/FFC-49

This page is intentionally left blank to maintain order of facing pages.

THE BEEMAN FORMATION (UPPER PENNSYLVANIAN) OF THE SACRAMENTO MOUNTAINS, NEW MEXICO: GUIDE TO THE DRY CANYON AREA WITH DISCUSSION ON SHELF AND BASIN RESPONSES TO EUSTASY, TECTONICS, AND CLIMATE

WILLIAM D. RAATZ[1] and J. A. (TONI) SIMO[2]
[1]ARCO Alaska, 700 G St., Anchorage, AK 99510;
[2]Department of Geology and Geophysics, University of Wisconsin-Madison, 1215 West Dayton St., Madison, WI 53706

Abstract—The Beeman Formation is an understudied Upper Pennsylvanian (Missourian, lower Virgilian), cyclic, mixed terrigenous clastic/carbonate unit that crops out in the Sacramento Mountains of south-central New Mexico providing three-dimensional dip-and-strike outcrop perspectives. The Dry Canyon area offers easily accessible exposures to the most basinward deposits of the upper Beeman Formation. Although thin, offshore, diastemic dark shales are present, the bulk of deposits in Dry Canyon consist of restricted high-energy limestones with abundant evidence for subaerial exposure. High-resolution sequence stratigraphy is possible within the Dry Canyon basin area and from the basin onto the shelf through correlation of maximum flooding surfaces, exposure surfaces, and biostratigraphy. Shelf deposits (e.g., Alamo Canyon) are composed of cyclic, massive, open-marine limestones separated by exposure surfaces. The paradoxical relationship of the basin deposits being dominated by high-energy, shallow-water restricted deposits and the shelf being dominated by open-marine limestones, a phenomenon here termed "inverse sedimentation," results from the interaction of high-frequency sea-level changes and basin geometry. Glacio-eustasy was responsible for most high-frequency vertical facies changes, while tectonics and climate controlled longer term trends in basin geometry and sediment type/paleosol development.

INTRODUCTION

The Sacramento Mountains in south-central New Mexico contain some of the most popularly visited exposures in the United States (Figs. 1 and 2). Of special interest are the excellent outcrops of highly cyclic, mixed carbonate/clastic Pennsylvanian strata. The Morrowan–Desmoinesian Gobbler Formation (Pray, 1952, 1961; Van Wagoner, 1977; Algeo et al., 1991) and the Virgilian Holder Formation (Cline, 1959; Pray, 1961; Wilson, 1967, 1972; Goldstein, 1986, 1988; Bachtel et al., 1997) have received the bulk of attention, while the Missourian Beeman Formation has largely languished, due in part to its recessive nature over much of the escarpment (Figs. 3 and 4). Pray (1952, 1961), Bergeron (1957), Wilson (1967, 1972), Schutter (1989), and Raatz et al. (1994, 1995, 1996) have specifically addressed the Beeman Formation, and only Pray (1952, 1961) and Raatz (1996) examined it in its entirety. This paper is derived from Raatz (1996) and represents the first published detailed sequence stratigraphic study of the Beeman Formation.

Since most groups only have the opportunity to examine the Beeman Formation at the Dry Canyon US-82 locality, this paper concentrates on providing a detailed description and interpretation for this location. However, summary discussions are provided regarding regional correlations and the unusual relationships between basin and shelf deposits.

Geography

The Sacramento Mountains comprise the eastern boundary of both the Rio Grande rift and the Tularosa Basin. The Tularosa Basin contains the White Sands National Monument and the city of Alamogordo (Fig. 1). Present topography results from a north-trending asymmetrically tilted fault block formed during Tertiary-Holocene extension. The fault block dips steeply to the west and gently to the east, creating a western escarpment with excellent exposures of Precambrian through Permian strata deeply dissected by a series of east–west canyons, providing an excellent opportuni-

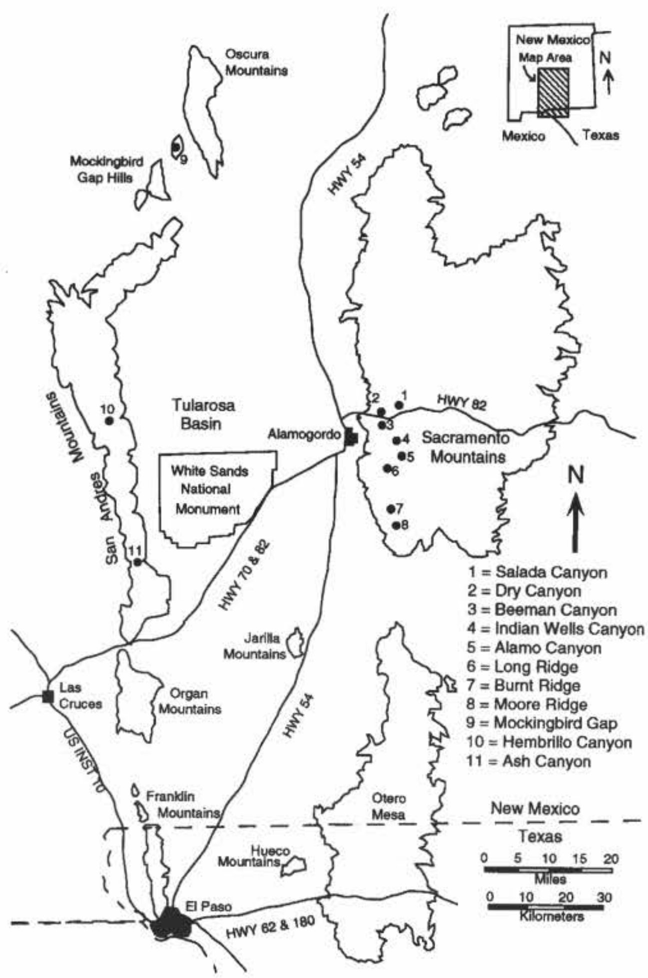

FIGURE 1. Regional context of the study area. Modified from Algeo et al. (1991).

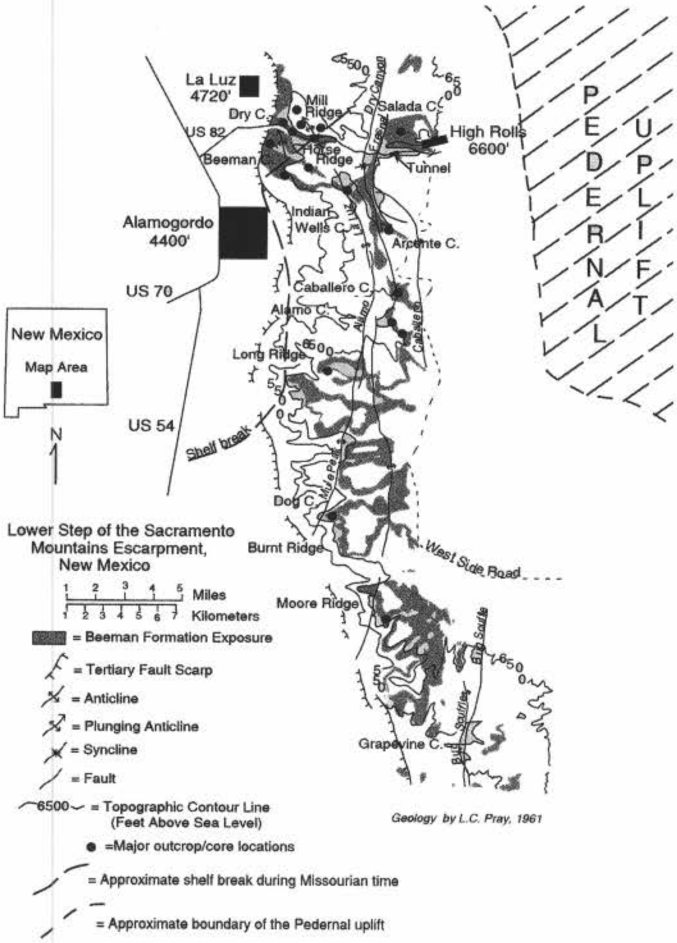

FIGURE 2. Structural map of the Sacramento Mountain escarpment, with the Beeman Formation outcrop belt shaded and locations of major outcrop/core measured section. The approximate positions of the Pedernal uplift and the shelf break during Missourian sea-level highstand are provided. Geology by Pray (1961).

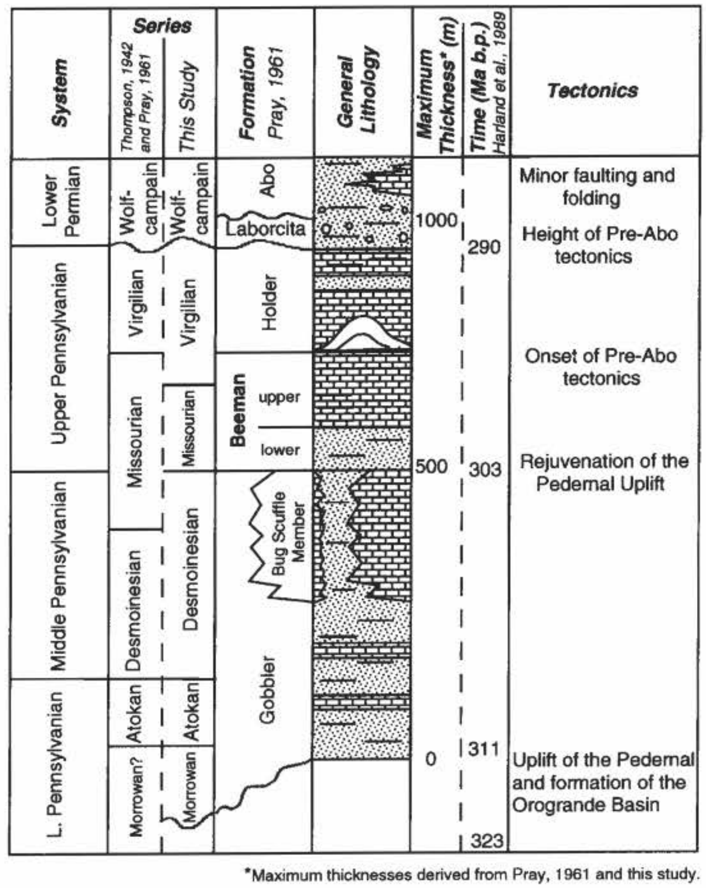

FIGURE 3. Stratigraphic column and tectonic events for the Pennsylvanian and lower Permian of the Sacramento Mountains.

ty to study three-dimensional depositional and stratigraphic relationships.

Deposits of Pennsylvanian age form over one-third of the exposed outcrop in the escarpment (~900 m; Pray, 1961). Access to many portions of the outcrop belt is difficult and time-consuming owing to the rugged topography and limited road system. An exception exists in Dry Canyon, which contains relatively good exposures and roadcuts with easy access along US-82.

Overview of the Paleozoic geologic setting of the Sacramento Mountain area

During the early to mid-Paleozoic the Sacramento Mountain area formed part of a stable, south-dipping ramp extending from the southern extreme of the Transcontinental Arch. Late Mississippian–Early Pennsylvanian compressional tectonics associated with the Appalachian Orogeny caused regional uplift, as recorded in the major unconformity at the Mississippi-Pennsylvanian boundary (Pray, 1961). This tectonism reactivated north-trending Precambrian lineaments (Kluth and Coney, 1981), and formed the Pedernal uplift and its conjugate basin, the Orogrande, separated by the narrow Sacramento shelf (Fig. 2). Pennsylvanian deposits in this newly formed basin record pulses of tectonic activity, high-frequency, high-amplitude, glacio-eustatic

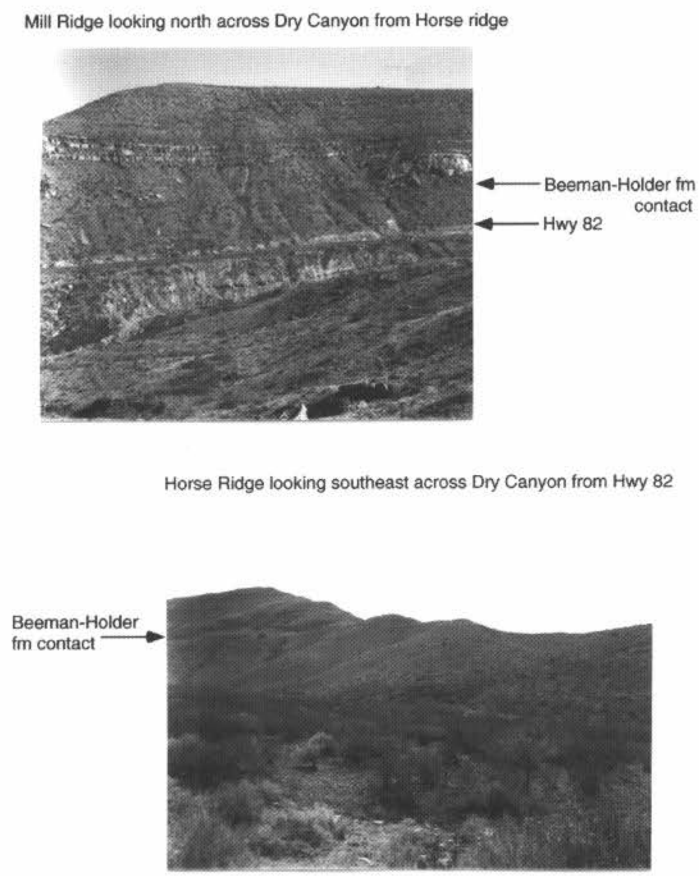

FIGURE 4. Photographs of Dry Canyon looking north toward Mill Ridge and southwest toward Horse Ridge. Hwy 82 = US-82.

TABLE 1. Lithofacies summary chart

Lithofacies	**Terrestrial Shale**	**Marine Shale**	**Terrestrial Siltstone**	**Marine Siltstone**	**Mixed Carbonate/Clastic**	**Calcareous Shale**
Code	tSh	mSh	tSlt	mSlt	C/S	CS
Mineralogy	Clay, quartz silt, mica, calcite	Clay, quartz silt, mica, calcite	Quartz silt, mica, calcite	Quartz silt, mica, calcite	Mono and polycrystalline quartz, plagioclase, feldspar, mica, calcite	Lime mud, quartz silt, mica
Grain Size/Texture	Clay	Clay	Silt	Silt	Usually medium, phi=1 to 2, angular to subrounded, moderately top poorly sorted	Clay
Flora and Fauna	Ostracodes, plants	Nautiloids, fish, Trepispira and Glyptomara gastropods, Idiognathodus and Streptognathodus conodonts, Dunbarella pectin	Plants	Rare conodonts, echinoderms, brachiopods, bryozoans, ammonoids, gastropods	Brachiopods, fusulinids, echinoderms	Branchiopods, ostracodes, plants
Structures		Lamination		Oscillatory ripples, bioturbation	Cross bedding	Bioturbation
Bedding Style	Fissile to blocky	Fissile	Thin, flaggy to massive	Flaggy to massive	Massive	Fissile to blocky
Vertical Associations	Af, Slt, CM	SLw, CM	tSh, CM, PFg, LLm	Af, CM	CS, LLm, SLw, TFB, Am	PFg, CM, Slt
Lateral Distribution	Throughout	Dry Canyon basin area	All but southern escarpment	Throughout	Mainly Dry Canyon basin area	Mainly Dry Canyon basin area
Depositional Environment	Floodplain	Deep marine, deposition below the pycnocline	Floodplain/overbank	Prodelta	Shallow marine: reworked lowstand terrestrial clastics and transgressive carbonates	Restricted lagoon to terrestrial
Lithofacies	**Carbonate Mudstone**	**Skeletal Limestone-wackestone**	**Skeletal Limestone-packstone**	**Skeletal Limestone-phylloid**	**Skeletal Limestone-grainstone**	**Peloidal Foraminiferal-wackestone**
Code	CM	SLw	SLp	SLph	SLg	PFw
Mineralogy	Lime mud	Lime mud, calcite, chert, dolomite	Lime mud, calcite, chert, dolomite	Lime mud, calcite	Calcite, dolomite, quartz silt	Lime mud, calcite
Grain Size/Texture	Mud	Wackestone	Packstone	Packstone	Grainstone	Wackestone
Flora and Fauna	Ostracodes, corals, bryozoans, brachiopods, gastropods, fusulinids, echinoderms	Ostracodes, corals, bryozoans, brachiopods, gastropods, fusulinids, echinoderms, foraminifera, holotheurian sclerites, trilobites, bivalves, phylloid algae, scaphopods	Ostracodes, brachiopods, echinoderms, foraminifera, gastropods, myalinids, trilobites, bivalves, phylloid algae, corals	Phylloid algae, foaminifera	Brachiopods, foraminifera, echinoderms, ostracodes, molluscs	Ostracodes, foraminifera, gastropods
Structures	Mudcracks, bioturbation	Bioturbation	Cross beds, fenestral porosity, rhizoliths, brecciation, mudcracks, bioturbation	Mound morphology	Cross beds, mudcracks, brecciation	Massive
Bedding Style	Thin to massive	Massive	Massive	Massive, mound	Massive	Massive
Vertical Associations	CS, PFg, SLw, Slt	Sh, CM, SLg, CS	SLg, CS, SLw, Slt	SLg, CM	CS, SLw, CM, SLp, Slt	PFg, CS, LLm, PFp, Slt
Lateral Distribution	Throughout	Throughout	Throughout	Mainly central escarpment	Throughout	Throughout
Depositional Environment	Marine: lagoon and below storm wave base	Open marine, below normal wave base	Marine: within storm to normal wave base	Open marine	Marine: normal wave base depths	Restricted marine: lagoonal
Lithofacies	**Peloidal Foraminiferal-packstone**	**Peloidal Foraminiferal-grainstone**	**Tubular Foram Boundstone**	**Laminated Limestone-muddy**	**Laminated Limestone-grainy**	**Brecciated Limestone**
Code	PFp	PFg	TFB	LLm	LLg	BL
Mineralogy	Lime mud, calcite	Calcite, dolomite, quartz silt	Lime mud, calcite	Lime mud, ciacite	Lime mud, calcite	Lime mud, dolomite, quartz silt, calcite
Grain Size/Texture	Packstone	Grainstone	Boundstone	Mudstone	Mudstone to grainstone	Mudstone to grainstone
Flora and Fauna	Ostracodes, foraminifera, tubular foraminifera, gastropods, brachiopod debris	Ostracodes, foraminifera, tubular foraminifera	Tubular foraminifera, foraminifera, gastropods, algae	Gastropods, ostracodes, foraminifera	Gastropods, ostracodes, foraminifera, tubular foraminifera	Matrix = foraminifera Clasts = foraminifera, ostracodes, moluscs
Structures	Cross beds, oscillatory ripple marks, rhizoliths, mud cracks, brecciation, bioturbation	Cross beds, oscillatory ripple marks, convolute bedding, rhizoliths, brecciation	Mudcracks, rhizoliths, differential compaction, brecciation	Lamination, dewatering structures, microfaults, flaser ripples, mud cracks, brecciation, wavy bedding, bioturbation	Lamination, graded beds, algal lamination, fenestral pososity, dewatering structures, mudcracks, flaser ripples, bioturbation	Brecciation, mudcracks, rhizoliths, blackened grains
Bedding Style	Massive	Massive	Lenticular to mound	Massive	Massive	Massive
Vertical Associations	CS, CM, PFw	CS, LLm, CM, PFw, Slt	CM, LLg, PFw	PFg, CS, LLg	LLm, PFg, Cs, Sh	PFg, LLm
Lateral Distribution	Throughout	Throughout	Mainly Dry Canyon basin area	Mainly Dry Canyon basin area	Mainly Dry Canyon basin area	Throughout
Depositional Environment	Restricted marine: normal wave base to peritidal	Restricted marine: normal wave base to peritidal	Restricted marine: Normal wave base to peritidal	Restricted marine: peritidal	Restricted marine: peritidal	Peritidal to terrestrial

sea-level fluctuations, and a climate change from equatorial wet to tropical seasonally wet-dry (Raatz, 1996). The narrowness of the shelf (3–5 km) created rapid lateral facies changes from inner shelf through basinal environments.

The lower Gobbler Formation consists of texturally and compositionally immature terrigenous clastics shed from the crystalline core of the Pedernal uplift (Meyer, 1966; Fig. 3). A rise of relative sea level and continued erosion reduced runoff from the highland clastic source and allowed cyclic, massive carbonates of the Bug Scuffle Member to be deposited across all but the central Alamo trough area, which contains clastic deltaic lobes (Pray, 1961; Van Wagoner, 1977; Algeo et al., 1991). A second pulse of tectonic activity further enhanced the relief of the Pedernal uplift during latest Desmoinesian through early Missourian time (Pray, 1961; Meyer, 1966). Immature terrigenous clastics covered the northern and central Sacramento shelf during this time (Kottlowski et al., 1956; Pray, 1961; Fig. 3). During middle through upper Missourian time tectonic quiescence (Raatz, 1996), generally high sea levels (Ross and Ross, 1987), and a drying climate (Philips and Peppers 1984; Raatz, 1996) resulted in cyclic carbonate deposition (Fig. 3), with thin-bedded, mixed carbonate/clastic cycles in the Dry Canyon basin area and massive, open-marine carbonate cycles on the shelf.

Compressional deformation beginning in the lower Virgilian, termed the "pre-Abo" event (Otte, 1959; Pray, 1961), created numerous north-trending faults and folds that affected deposition of the uppermost Beeman, Holder, and Laborcita Formations (Figs. 2 and 3). In Dry Canyon, the rise of the La Luz anticline created high-energy, restricted environments near its crest that overprinted glacio-eustatic sea-level changes during uppermost Beeman Formation deposition (Wilson, 1967, 1972; Raatz, 1996). The Virgilian Holder Formation marks a return to deeper water, more cyclic deposition in which the anticline acted as a shelf break over which large, reservoir analog phylloid algae mounds prograded basinward (Wilson, 1967, 1972). The Orogrande Basin was filled entirely during the Wolfcampian and became part of the Permian Northwest Shelf area (King, 1942; Pray, 1961).

DRY CANYON

Geography and location of outcrops

The mouth of Dry Canyon is located just northeast of the city of Alamogordo between Mill and Horse ridges (Figs. 2, 4, and 5). When traveling east from Alamogordo toward the mountains on US-82, the westernmost in situ outcrops and roadcuts encountered are of the upper Beeman Formation carbonates, with the lower Beeman Formation sandstones only exposed along the western side of Mill Ridge near La Luz. This is a locally exhumed anticlinal crest on Horse Ridge, and in Beeman Canyon and areas southward (Figs. 3 and 5). US-82 largely follows a single stratigraphic level as

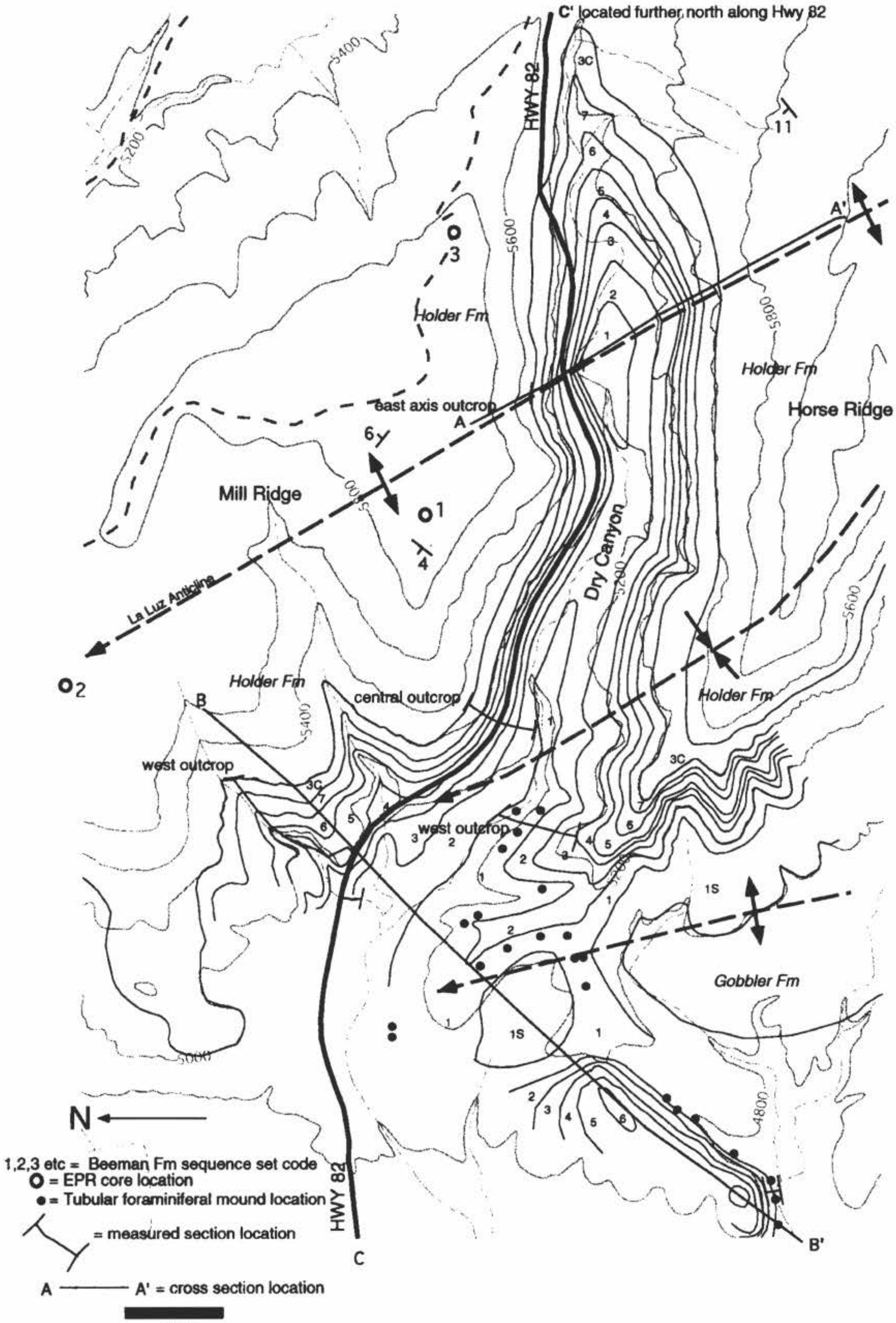

FIGURE 5. The Dry Canyon area with individual sequence sets from the upper Beeman Formation mapped, along with the location of measured sections, tubular foraminiferal, Leopard-rock mounds, and cross sections. Note that C' is located north of the mapped area. The code numbers on the map correspond to the following: 1S = super-sequence set 1S, 1= sequence set 2C-1, 2 = 2C-2, 3 = 2C-3, 4 = 2C-4, 5 = 2C-5, 6 = 2C-6, 7 = 2C-7, 3C = super-sequence set 3C. Unit 4C is below map resolution and included within 3C. Due to the extensive amount of cover in this area, the map is an approximation based on the detailed measured sections, observations made while walking the entire area, and geometric relationships derived from unit thicknesses and structural dips.

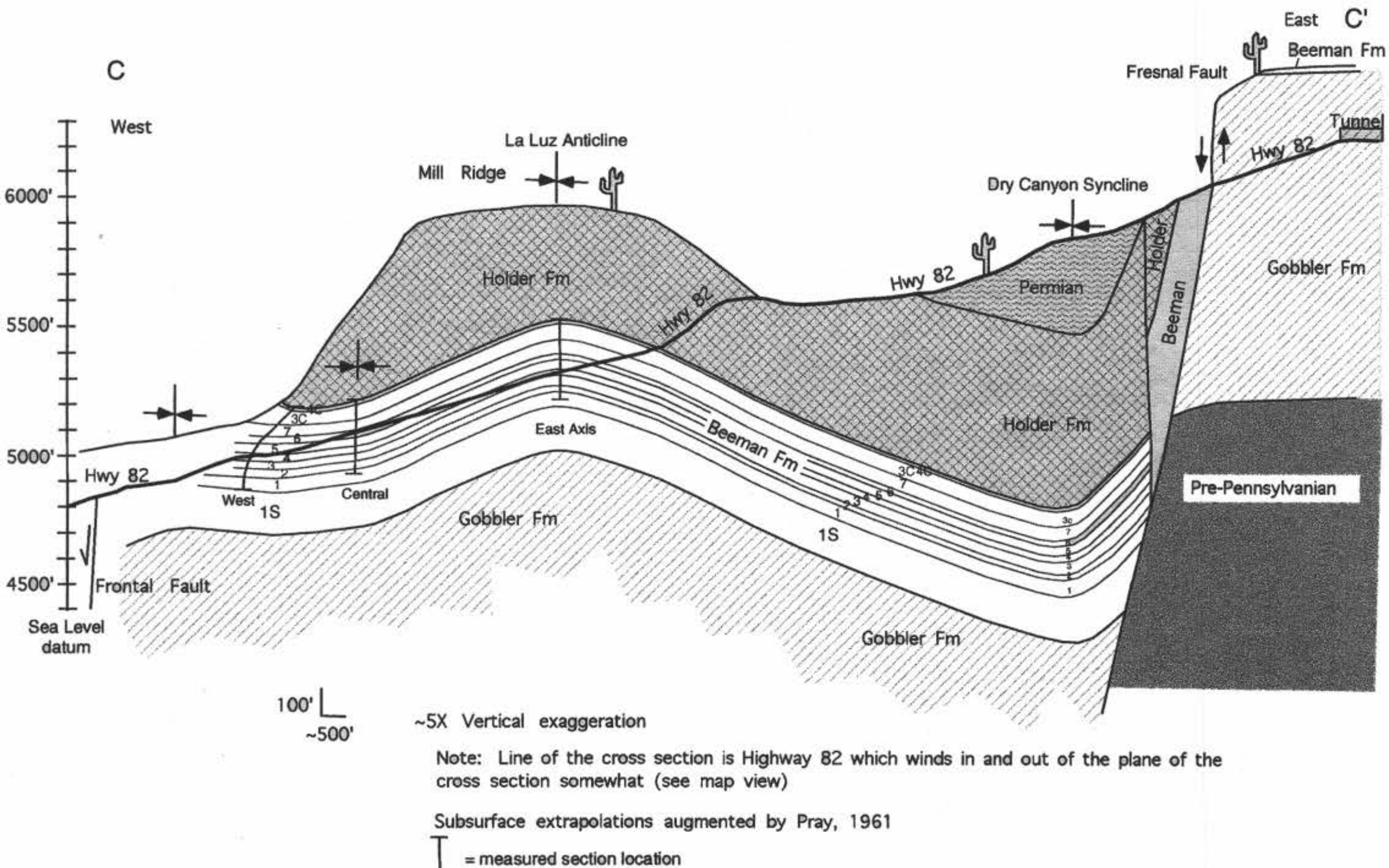

FIGURE 6. East–west cross section through Dry Canyon along US-82. The unit codes follow those in Figure 5, with the exception that 4C is here broken out as a separate unit.

it ascends the western flank and approaches the crest of the La Luz anticline (Figs. 4, 5, 6, and 7). After the crest, it quickly passes through the more massive carbonates of the uppermost Beeman Formation that comprise the eastern-dipping flank of the structure. The highway continues through exposures of east-dipping Holder Formation. The topography then flattens and the canyon opens as the highway passes into the broad, north-trending Dry Canyon syncline with Permian Abo and Laborcita Formation redbeds and carbonates exposed (Fig. 6). Just west of the Lincoln National Forest US-82 tunnel, west-dipping Permian redbeds, followed by Holder Formation carbonates and redbeds and Beeman Formation carbonates and green sandstones, are exposed in steeply dipping beds within the eastern flank of the Dry Canyon syncline (Fig. 6). These outcrops are contorted and largely incomplete due to the deformation caused by the Fresnal fault, which uplifts the massive Desmoinesian Bug Scuffle limestones ~365 m to form the dramatic cliffs at and east of the tunnel (Pray, 1961; Fig. 6).

The Beeman Formation in Dry Canyon

The Dry Canyon area contains the most basinward outcrops of the Beeman Formation in the Sacramento Mountains. From most basinward to more shelfal, these basinal localities include: Dry Canyon core #2, Dry Canyon west outcrop, Dry Canyon central outcrop, Dry Canyon core #1, Dry Canyon core #3, and Dry Canyon east axis outcrop (Figs. 5 and 8). Although upper Beeman Formation exposures are relatively good in Dry Canyon, individual bed tracing is only rarely possible for any significant distance. Therefore, vertical measured sections have been correlated using biostratigraphy, lithostratigraphic characteristics (e.g., exposure surfaces, maximum flooding surfaces), stratigraphic stacking patterns, and inferred position based on thickness and strike and dip.

Lithofacies

This study has recognized 18 lithofacies (Table 1) in the Beeman Formation, and has interpreted their significance with regard to depositional environments, paleowater depths of deposition (Fig. 9), and cyclicity. Although we agree with previous workers (Pray, 1961; Meyer, 1966; Wilson, 1967, 1972) that the Dry Canyon area represents a basinal position, we disagree with Pray's (1961) and Wilson's (1967, 1972) interpretation that the majority of preserved Dry Canyon strata were deposited in offshore environments. Rather, we contend that the majority of preserved strata represents highly restricted shallow-water to peritidal environments of deposition, with abundant evidence for high-energy rip-ups, winnowed high-energy fabrics, peritidal lamination, a restricted low-diversity fauna, and subaerial exposure. The basinal nature of the area is only recorded in thin (<1 m) transgressive and maximum-flooding deposits consisting of diastemic dark shales, skeletal wackestones, and some of the carbonate mudstones.

A typical unconformity-bounded lithofacies cycle assemblage is strongly asymmetric, with a variably present, thin (~0.1 m), basal-transgressive clastic unit composed of reworked terrestrial material followed by a thin (~0.2–0.5 m) transgressive wackestone with open-marine fauna. This is followed by a thin (~0.3 m) diastemic, maximum-flooding dark shale variably containing pelagic nautiloids, gastropods, pectin, fish, and conodonts. A regressive wackestone (~0.2–2 m) typically overlies the offshore shale, overlain by a thick (~10–15 m), restricted, regressive, peloidal foraminiferal

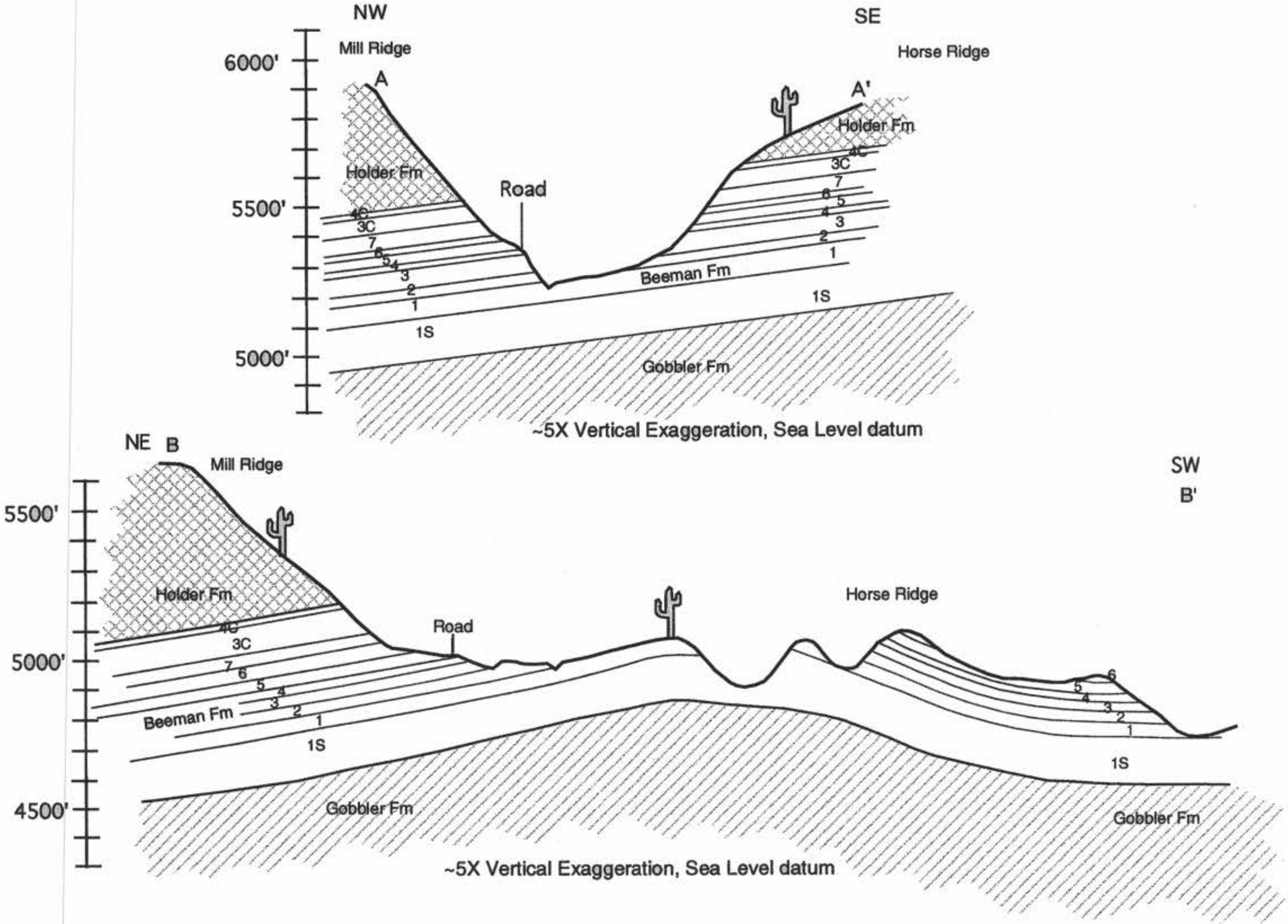

FIGURE 7. Generally N–S cross sections across Dry Canyon and Mill and Horse ridges. Cross section A–A' follows the axis of the La Luz anticline, while B–B' is located closer to the mouth of the canyon.

grainstone with interbedded laminated peritidal limestones and barren calcareous shales. The regressive package is capped by subaerial exposure, including rhizoliths, mudcracks, caliche, autobrecciation, and circumgranular cracking. The entire open-marine assemblage of lithofacies may therefore only consist of ~10% of the cycle.

Sequence stratigraphic framework

The lithofacies (Table 1) in conjunction with significant surfaces of subaerial exposure and flooding are grouped into a hierarchy of sequence stratigraphic units, including parasequences, parasequence sets, sequences, sequence sets, and super-sequence sets. The mappable unit is the sequence set (Fig. 5). The goal of the sequence stratigraphic study is to create a nested hierarchy of genetically related, chronostratigraphically significant units (e.g., Van Wagoner et al., 1990). Their recognition provides a detailed framework for the interpretation of depositional environments and the determination of depositional controls.

Figure 8 illustrates the correlation between core and outcrop measured sections for the Dry Canyon area. Below is a brief description of each defined unconformity-bounded sequence: the coding system used to name sequences consists of the super sequence set number and its primary lithology (S for sandstone, C for carbonate), followed by a dash and the sequence set number followed by a letter designating the sequence. In addition, sequences are defined as "major," "intermediate," and "minor" after Midcontinent terminology (e.g., Boardman and Heckel, 1989), referring to whether their maximum flooding deposit is a diastemic, offshore dark shale (major), an open-marine wackestone (intermediate), or some more restricted lithology (minor). The lower Beeman Formation siliciclastic-dominated 1S super sequence set (Fig. 3) is not discussed here because it is not encountered in Dry Canyon.

Sequence 2C-1a

Major sequence 2C-1a ranges from 3 to 9 m in thickness, contains three to four parasequences, and forms the lowermost carbonate-dominated unit (Fig. 8). The base of this sequence in Dry Canyon core #2 contains a thin (~5 cm), pyritized myolinid layer followed by an offshore dark shale. Dry Canyon cores #1 and #3 do not contain the myolinid lag, but instead have terrigenous clastics at their bases. In addition, updip locations contain thin skeletal wackestones but no dark offshore shales. The sequence is capped by restricted carbonates with the upper ~1 m containing subaerial

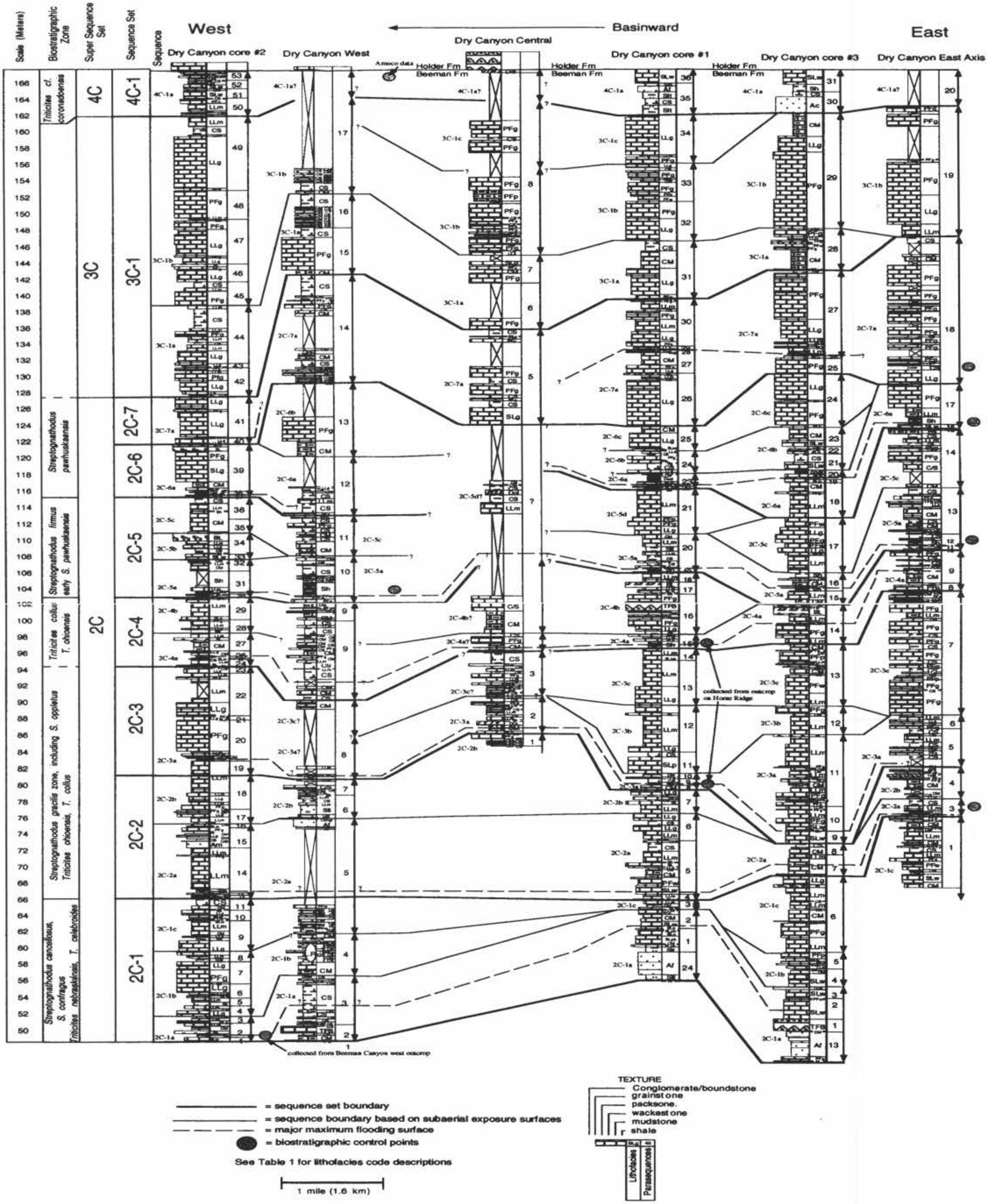

FIGURE 8. Detailed measured sections for the upper Beeman Formation in Dry Canyon with exposure surfaces and maximum flooding surfaces correlated. The columns to the right of each lithic column represent lithofacies codes (see Table 1) and parasequences, while the arrows delineate individual sequences. The location of each section is provided on Figure 5, and the key to lithologies are given in Figure 10. Datum is the Beeman-Holder formational boundary.

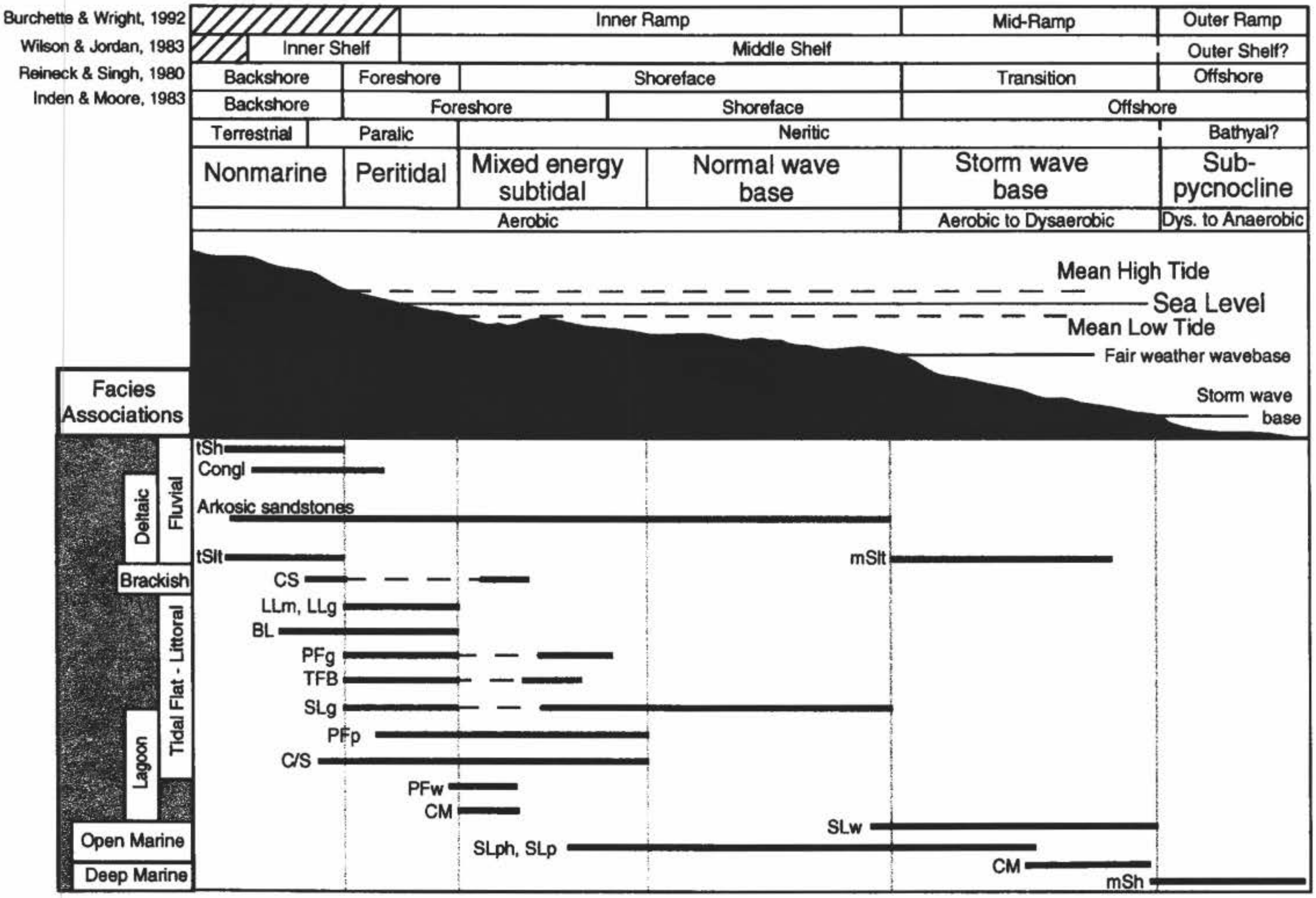

FIGURE 9. Interpreted bathymetric range for deposition of the major lithofacies described in the Beeman Formation.

exposure features, including rhizoliths, mudcracks, circumgranular cracking, and auto brecciation.

The basal sandstones indicate sedimentary bypass in the updip sections. The myolinid layer is interpreted as a transgressive lag, and the dark offshore shales and updip equivalent wackestones represent maximum flooding. Along the remaining escarpment, the thickness of 2C-1a greatly expands, forming a major cliff visible throughout most of the central Sacramento Mountains.

Sequence 2C-1b

Intermediate sequence 2C-1b ranges from 4 to 8 m in thickness and contains one to five parasequences (Fig. 8). The number of parasequences generally decreases updip, consistent with depositional pinch-out. The sequence is composed largely of restricted limestone, including LL, PFg, and tSlt. A thin bed forms the maximum-flooding deposit, and the sequences is capped by thick package of restricted limestones with subaerial exposure features. Tubular foraminiferal mounds (Leopard rock) near the top of this sequence form a discontinuous but laterally extensive marker in Dry and Beeman Canyons. The lateral thickness changes and general discontinuity of this sequence (Fig. 8) in the basin suggest erosion occurred during deposition of the high-energy peritidal deposits, completely eroding the sequence locally.

Sequence 2C-1c

Sequence 2C-1c is also an intermediate sequence that varies from 1 to 9.5 m thick (Fig. 8), and contains one to three parasequences, again with the number of parasequences generally decreasing shelfward as the sequence pinches out updip. The sequence is dominated by restricted peritidal deposits with only a thin SLw maximum flooding unit. It is capped by subaerial exposure.

Sequence 2C-2a

Major sequence 2C-2a marks the return of marine conditions across the entire basin. Thickness of the sequence varies from 4 to 10 m and it contains from two to five parasequences. The most basinward Dry Canyon area, core #2, contains an offshore shale that correlates updip to thin marine shales and open-marine limestones in cores #1 and #3 (Fig. 8), as well as an offshore shale in the Dry Canyon east section, suggesting that the shale's absence downdip may be erosional. A coarse-grained arkose unit occurs near the top of the sequence in the most basinward core #2 and Dry Canyon west outcrop. The sequence is capped by thick peritidal laminites and exposure features.

Sequence 2C-2b

Intermediate sequence 2C-2b varies in thickness from 3 to 6.5 m (Fig. 8), and contains one to five parasequences. It is composed almost exclusively of peritidal carbonates, with only a thin open-marine limestone maximum flooding deposit near the base of the most basinward core #2 section. Again, the number of parase-

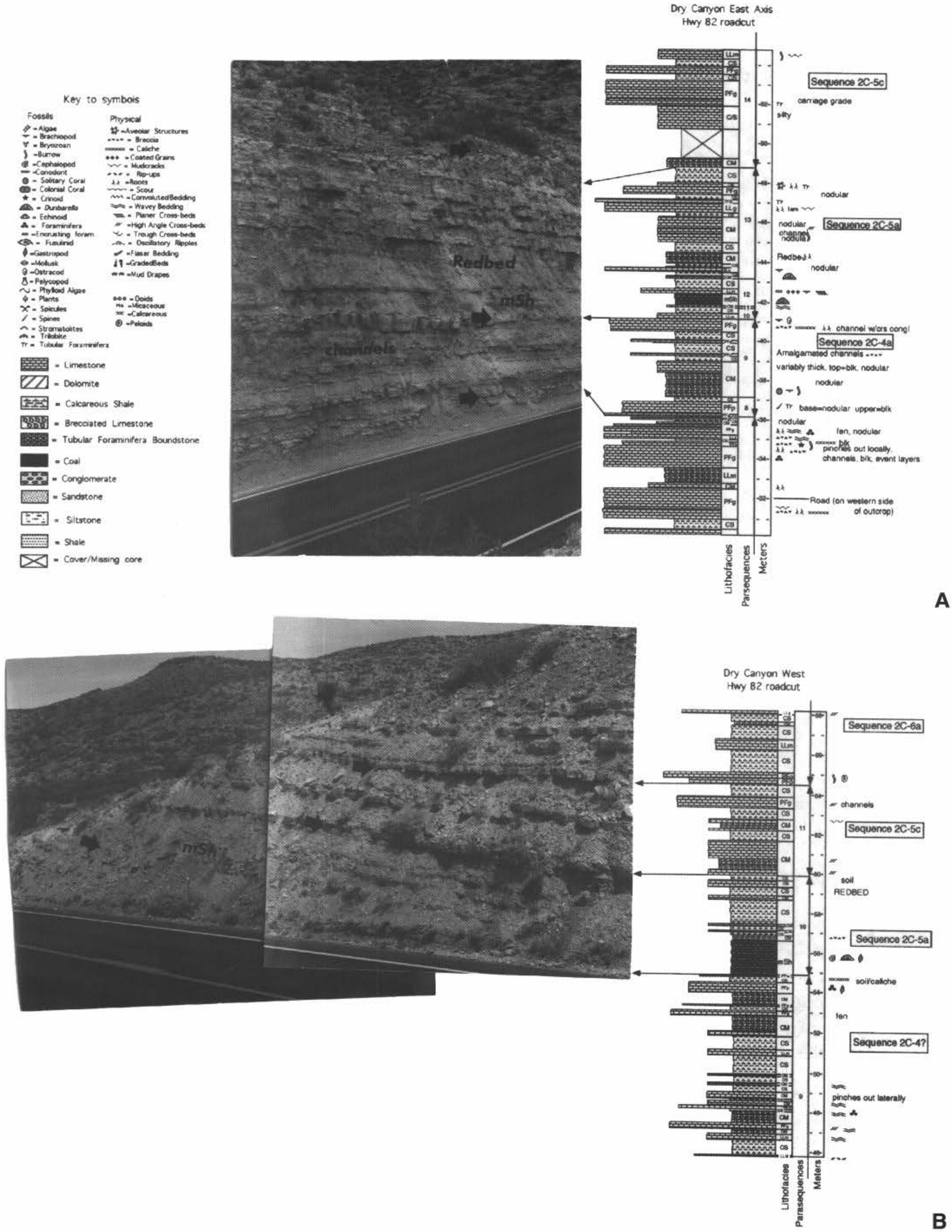

FIGURE 10. Outcrop photos of the US-82 roadcuts in Dry Canyon with accompanying measured sections. 10A is the Dry Canyon east axis roadcut on the La Luz anticlinal axis, and 10B is the westernmost roadcut, Dry Canyon west. Arrows mark sequence boundaries.

quences decreases updip consistent with an updip depositional pinchout.

Sequence 2C-3a

Major sequence 2C-3a varies in thickness from 2 to 14 m (Fig. 8), with two to five parasequences. The offshore shale is well-developed in the most basinal core #2, but becomes progressively thinner and less well-developed updip through core #3. Updip of core #3 it pinches out altogether. The open-marine component of the sequence is thin (~1 m), while the remainder of the sequence is composed of high-energy peritidalites. The sequence is unusually thin in the central basin cores #1 and #3 area, perhaps due to erosion. The sequence is capped by laminites, tubular foraminiferal units, breccia, mudcracks, and rhizoliths.

Sequence 2C-3b

Intermediate sequence 2C-3b occurs only in the central portion of the basin (cores #1 and #3). It varies from 3.5 to 7 m in thickness (Fig. 8), and contains one to four parasequences. In core #1, 2C-3b contains a thin SLp maximum flooding deposit overlain by thick laminites capped by exposure. Updip in core #3 the sequence is composed exclusively of laminites and restricted limestone capped by exposure.

Sequence 2C-3c

Minor sequence 2C-3c varies from 7 to 15 m thick (Fig. 8) and contains one to two parasequences. It occurs only in the Dry Canyon central outcrop, core #1, core #3, and Dry Canyon east outcrop. It is composed exclusively of restricted carbonates with the exception of a thin phylloid algae-bearing unit in core #1. Rhizoliths and nodular caliche cap the sequence.

Sequence 2C-4a

Major sequence 2C-4a is generally thin, varying from 2 to 7 m, and contains one to four parasequences (Fig. 8). Thin to absent open-marine limestones bound an offshore black shale in the most basinward core #2 and core #1 sections, while in Dry Canyon east outcrop an open-marine limestone is the maximum flooding deposit. Core #3 contains no open-marine unit whatsoever. A mixture of restricted low-energy lagoonal and high-energy peritidal deposits form the remaining section, with breccia, nodular caliche, and rhizoliths capping the sequence.

Sequence 2C-4b

Sequence 2C-4b is an intermediate sequence ranging from 4.5 to 8 m in thickness (Fig. 8). It is largely covered by debris in outcrop due to its position at and directly below US-82. In cores #2 and #1 the sequence is dominated by tSlt and restricted limestone, including breccia, leopard rock, laminites, and PFg. Only a thin skeletal limestone maximum flooding deposit is preserved at the base of the sequence.

Sequence 2C-5a

Major sequence 2C-5a varies from 3.5 to 7.5 m thick, contains one to four parasequences, and is the stratigraphic unit exposed along US-82 for the majority of its length on the western limb of the La Luz anticline (Figs. 5, 6, 8, and 10). The maximum-flooding offshore shale contains a diverse pelagic fauna, including abundant conodonts, nautiloids, and *Trepospira* gastropods, and is the first offshore shale to be preserved throughout the entire basin area. Thin SLw deposits bound the mSh, with the regressive SLw overlain by restricted limestone and a thick red tSh paleosol with nodular caliche. Numerous scour and channel deposits also occur in the upper part of the sequence.

Sequence 2C-5b

Intermediate sequence 2C-5b represents a sea-level rise that only drowned the most basinward core #2 locality, where it is 3 m thick and contains two parasequences (Fig. 8). It is composed of a thin, lower skeletal limestone maximum-flooding unit overlain by a thicker restricted limestone cap containing breccia and mud cracks.

Sequence 2C-5c

2C-5c is an intermediate sequence that varies from 4.5 to 7 m in thickness and contains one to two parasequences (Fig. 8). It contains a thin open-marine limestone maximum-flooding unit in only the most basinward core #2 and Dry Canyon west outcrop, while the more updip sections contain only high-energy restricted peritidal units. The sequence is capped by scour, channel forms, mudcracks, and rhizoliths.

Sequence 2C-5d

2C-5d is a minor sequence that occurs sporadically in the basin area. It is up to 5.5 m thick and contains one parasequence (Fig. 8). No open-marine components were observed, and the sequence is dominated by laminites and PFg, and capped by breccia and mud cracks.

Sequence 2C-6a

Major sequence 2C-6a ranges from 2 to 7.5 m in thickness and contains one to three parasequences (Fig. 8). An offshore mfs shale occurs in all Dry Canyon localities, bounded by thin open-marine limestone beds. The mSh is closely overlain by a coal bed in cores #1 and #3, while in core #2 a plant-rich calcareous mudstone overlies the mfs. A coarse-grained arkose unit exists only in an extreme western outcrop downdip of the core localities, probably representing a local channel preserving evidence of sedimentary bypass of the shelf and eastern basin. The sequence is capped either by the coal unit or peritidal carbonates with rhizoliths.

Sequence 2C-6b

2C-6b is an intermediate sequence that varies from 3 to 9 m in thickness and contains one to three parasequences (Fig. 8). Thin mfs open-marine limestones are overlain by thick restricted carbonates and capped by exposure.

Sequence 2C-6c

2C-6c is an intermediate sequence occurring only on cores #1 and #3. It is 3.5–6.5 m thick and contains one parasequence (Fig. 8). Its thin skeletal limestone mfs unit, where present, is overlain by high-energy carbonates capped by exposure, including rhizoliths and mud cracks.

Sequence 2C-7a

Major sequence 2C-7a varies from 6 to 18 m in thickness and contains one to five parasequences (Fig. 8). The maximum flooding deposit consists of a poorly developed offshore shale surrounded

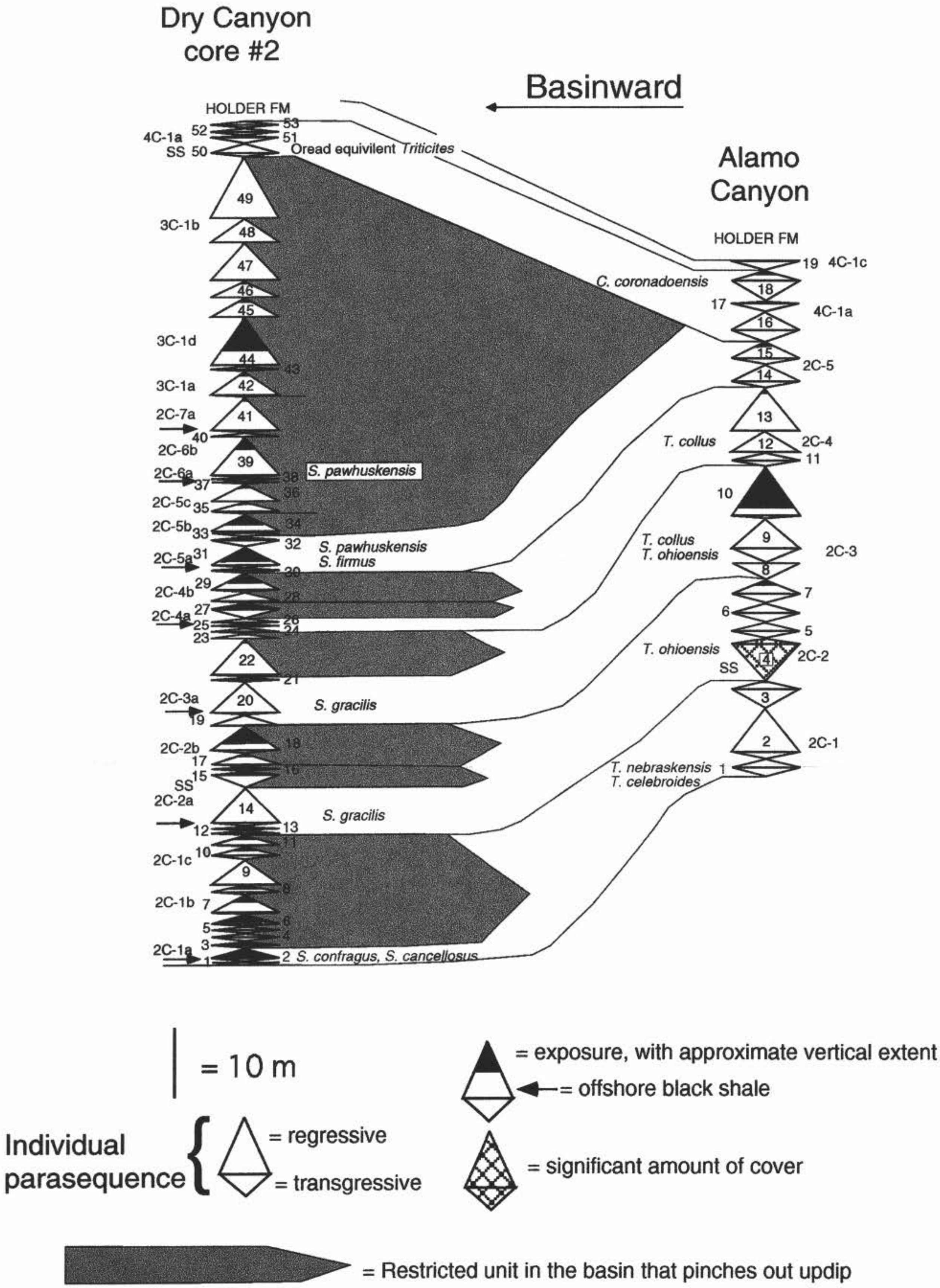

FIGURE 11. Correlation of the upper Beeman Formation from basin (Dry Canyon core #2) to shelf (Alamo Canyon) environments. Note that the parasequences and sequences thicken and decrease in number updip. Only the major sequences containing a deep-water dark shale in the basin are present on the shelf. The shaded areas represent restricted basinal strata that pinch out updip.

by thin skeletal limestones. The shale is unusually well developed in the middle basin core #1 and #3 area relative to the deeper basin core #2. The sequence is capped by high-energy carbonates with exposure evidence.

Sequences 3C-1a through 3C-1c

Sequence set 3C-1 is a thick unit (up to 40 m; Fig. 8) composed almost entirely of high-energy restricted carbonates with essentially no open-marine components. Exposure features, perhaps laterally continuous, occur at approximately similar stratigraphic levels and have been correlated as sequence boundaries, but without definable maximum flooding units these sequences are suspect. The lower portion (sequence 3C-1a) appears to record a slightly higher sea level than the remaining sequence set, as it contains a poorly developed open-marine unit. 3C-1 is replete with clastic sedimentary structures, including crossbeds, ripple marks, and convolute bedding. Numerous stacked carbonate channels are exposed on the north side of Horse Ridge and in the upper reaches of eastern Beeman Canyon. This sequence set contains Wilson's (1967, 1972) prograding oolitic shoal marker bed, evidence of active uplift of the La Luz anticline during this time.

Sequences 4C-1a through 4C-1c

Incomplete sequence set 4C-1 is only ~5 m in thickness in the basin (Fig. 8), and contains two to four parasequences. It contains a basal tan arkose that was mapped in detail by Wilson (1967, 1972), who determined it to represent a shoal on the axis of the emerging La Luz anticline. The sandstone forms the base of a significant deepening event that deposited open-marine wackestones across the Dry Canyon area and provided accommodation space for the large phylloid algae mounds of the Holder Formation. The base of these mound complexes define the Beeman-Holder formational boundary.

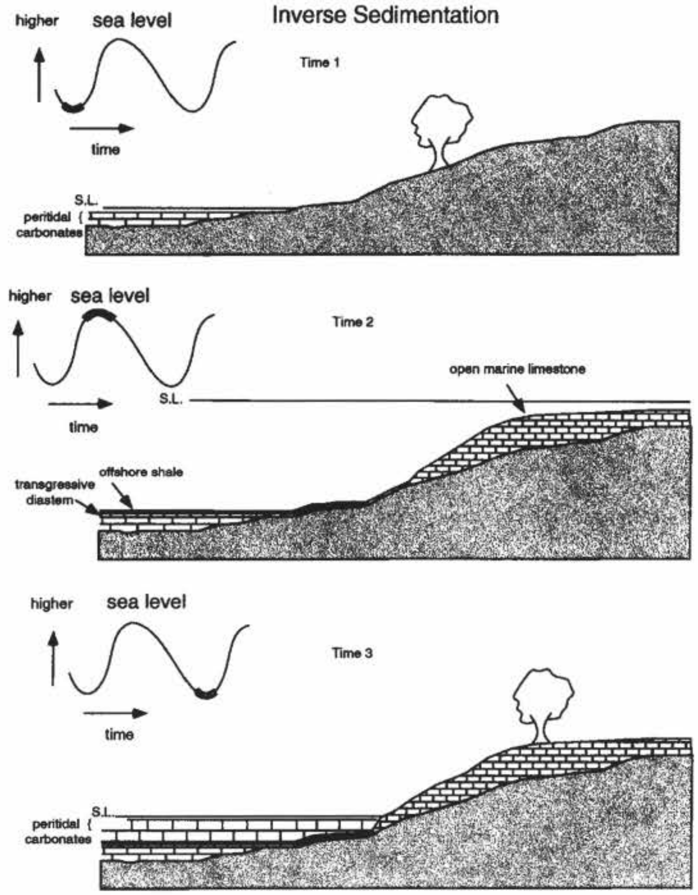

FIGURE 12. Schematic model of how basin geometry and sea-level changes created "inverse sedimentation" in the upper Beeman Formation, with high-energy restricted deposits dominating the basin and open-marine limestones dominating the shelf.

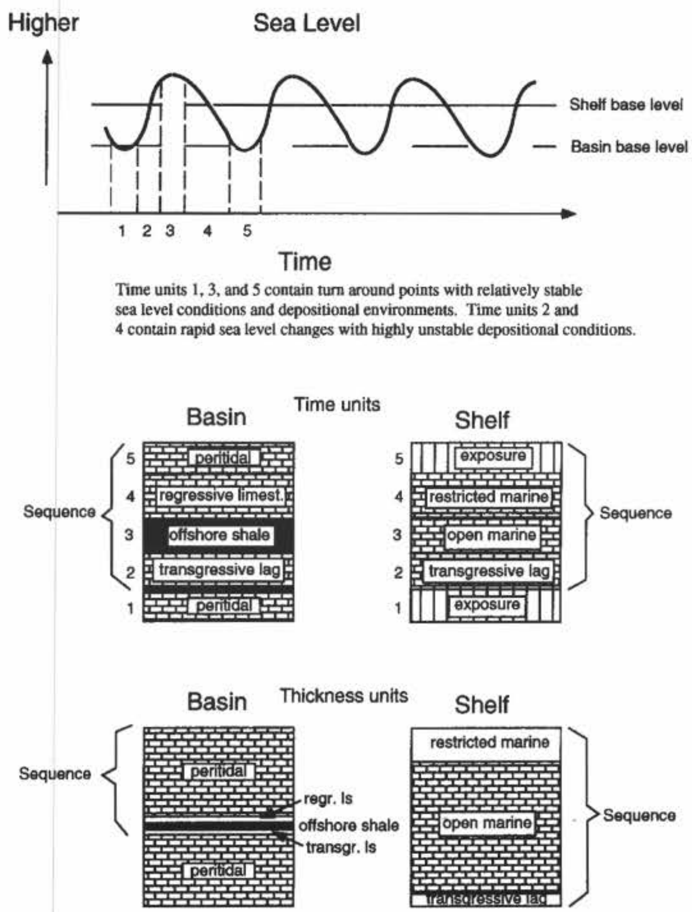

FIGURE 13. Basin vs. shelf responses to high-frequency sea-level changes in both time and depth units illustrating "inverse sedimentation" for the upper Beeman Formation.

SHELF TO BASIN CORRELATION OF THE BEEMAN FORMATION

The interaction of glacio-eustasy, tectonics, climate, and basin geometry create a complicated depositional and stratigraphic pattern in the Beeman Formation (Raatz, 1996). Volumetrically, the Dry Canyon basinal area is dominated by restricted peritidal deposits, whereas the updip shelf areas (e.g., Alamo Canyon) are dominated by open-marine limestones. This paradoxical relationship, here termed "inverse sedimentation," can be explained through detailed biostratigraphy and correlation of exposure and maximum flooding surfaces across major facies changes.

In sequence sets 2C-1 through 2C-5, thin, basinal, diastemic limestone lags and dark offshore shales in Dry Canyon correlate updip in Alamo Canyon to thick, massive, open shelf carbonates, while peritidal deposits in the basin correlate to exposure updip on the shelf (Fig. 11). Only the major sequences, representing less than half of the total parasequences and sequences recorded in the basin, contained sufficiently high sea levels to reach the shelf. On the shelf, these major sequences deposited thick open-marine limestones that are coeval with the thin, diastemic basin dark shales. Despite containing offshore shales in the basin, sequence sets 2C-6 and 2C-7 are not present on most of the shelf, due either to nondeposition or erosion following the extended period of exposure during 3C time.

The thick, restricted, high-energy sequence set 3C-1 carbonate unit is only present in the basin area and locally the outer shelf, and correlates to exposure updip (Fig. 11). The 4C unit capping the Beeman Formation thickens on the shelf and contains additional sequences that are correlatable to the lower Holder Formation phylloid algae mounds in the basin (Table 2). This indicates that although the mounds locally prograded basinward off of the axis of the La Luz anticline in the Dry and Beeman Canyons area (Wilson, 1967, 1972), the lower Holder Formation itself retrograded updip, defining a generally transgressive pattern of relative sea level during lower Virgilian time. This indicates that the Beeman-Holder formational boundary becomes younger updip.

Inverse sedimentation

"Inverse sedimentation" is defined by this study to explain the paradoxical relationship found in super sequence set 2C of the Beeman Formation, in which the basin contains a higher volume of shallow, restricted marine deposits and subaerial alteration than shelfward deposits. This concept is significant because an improper understanding of this inversed relationship led previous workers to interpret the Dry Canyon tidalites and restricted marine deposits as deep water sediments (Pray, 1961; Wilson, 1967, 1972), based partly on the fact that they were basinward of known open-marine shelf deposits. Mistakes resulting from this incorrect inference may not be unique to the Sacramento Mountains. In addition, if this had been a frontier area with only limited data available (e.g., no outcrops and only one core from Dry Canyon and one core from Alamo canyon), it would have been natural to misinterpret the entire shelf-to-basin trend as being west to east rather than east to west. Only recognition of the thin diastemic offshore dark shales provide the clue necessary to properly interpret the trend.

Inverse sedimentation in the Beeman Formation largely resulted from the interaction of basin geometry and high-amplitude, high-frequency, glacio-eustatic sea-level changes. The sea-level changes approximated the shape of an asymmetric sine wave, with rapid sea-level change where the slope of the curve was steep, and slow changes near the turn around apexes where the curve was of low angle or flat (Figs. 12 and 13). At the lowest node of the sea-level curve, a stable, restricted, shallow-water environment existed in the Dry Canyon basin area, resulting in the deposition of peritidal carbonates. The shelf was exposed during this time, resulting in the formation of laminar caliche. Rapid sea-level rise ensued, depositing only thin transgressive lag deposits across the basin and locally on the shelf. At maximum flooding, the flat-to-low angle upper apex of the sea-level curve again created stable environments, with thin, diastemic sub-pycnocline offshore shales deposited in the basin and thick open-marine limestones on the shelf (Figs. 12 and 13). Subsequent sea-level fall deposited a regressive limestone across the shelf and basin, re-exposed the shelf area, and filled the limited accommodation space in the Dry Canyon basin area with peritidal limestones. This scenario cyclically repeated with each glacio-eustatic sea-level change and created a scenario where basinal peritidal carbonates are correlative to exposure surfaces updip, and thin offshore shales are correlative to thick open-marine limestones updip, with an overall basin section dominated by shallow peritidal carbonates, and a shelf section dominated by deeper open-marine limestones (Figs. 12 and 13).

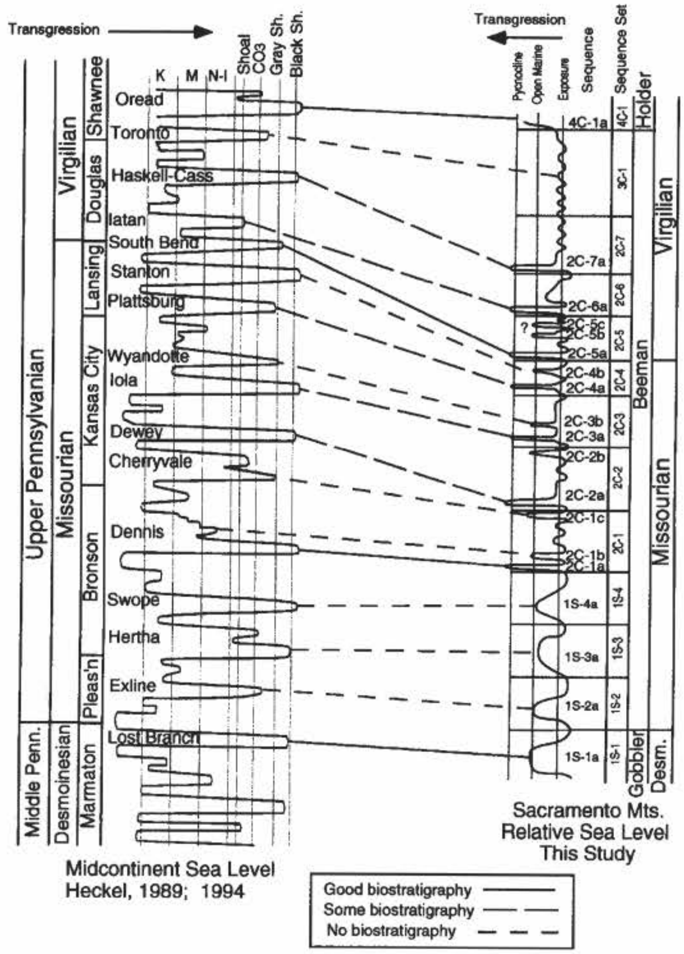

FIGURE 14. Correlation of the relative sea-level curve from the Beeman Formation of the Sacramento Mountains to the largely eustatic curve of the Midcontinent. The quality of the Sacramento Mountain biostratigraphy used to make the correlations is noted. Where the curves are similar (e.g., sequence set 2C) glacio-eustatic forces are interpreted to control Beeman Formation deposition, whereas deviations (e.g., sequence set 3C) represent overprinting by tectonics.

Non-Waltherian stratigraphic relationships

Walther's Law states that facies occurring in a conformable vertical succession had, at one instant in time, also occurred as laterally contiguous facies. Abrupt changes in vertical facies not consistent with Walther's Law have been interpreted to result from rapid glacio-eustatic sea-level changes and are characteristic of deposits of Pennsylvanian age throughout North America (e.g., Soreghan, 1992). The suggested explanation for non-Waltherian stratigraphic stacking is that sea-level changes were sufficiently rapid that non-equilibrium conditions prevailed, resulting in nondeposition. This is an especially valid concern regarding carbonates, where facies do not migrate by pure physical mechanisms, but must migrate through re-establishment of entire biological communities and ecosystems, a delicate balance that takes time.

In the Dry Canyon basin area, the Beeman Formation super-sequence set 2C contains subaerial exposure surfaces often overlain by very thin transgressive lags (cm scale) and thin transgressive open-marine limestones (cm to decimeter scale), followed by the offshore shale, a regressive limestone, and a thick package of restricted limestones including numerous exposure events. The transgressive or regressive limestones may be missing in any given sequence, however, resulting in the offshore shale being in direct

TABLE 2. Biostratigraphic correlations from shelf to basin and to the Midcontinent.

Fusulinacean Zone: Wilde (1990)	Fusulinacean Zone: Ross and Ross (1987)	Conodont Zone	Approximate Midcontinent equivilent cyclothem	Sacramento Mts fauna: Basin	Sacramento Mts fauna: Shelf	Sac. Mts sequence number
VC-1	V2	*S. zethus*	Oread	Oread equiv. *Triticites*	*T. cf. coronadoensis*	Holder Fm 4C-1
MC-4	V1	*S. zethus*	Toronto			3C-1a
			Haskell-Cass		Not Present	2C-7a
MC-3	M6	upper *S. pawhuskensis*	Iatan	*S. pawhuskensis*		2C-6a
		lower *S. pawhuskensis*	South Bend	early *S. pawhuskensis* *S. firmus*		2C-5a
		S. firmus	Stanton			2C-4b
	M5	*S. gracilis* upper	Plattsburg		*T. cf. collus*	2C-4a
			Wyandotte	*S. gracilis* -types		2C-3b
MC-2	M4		Iola		*S. oppletus* *T. collus* *T. ohioensis*	2C-3a
		S. gracilis middle	Dewey		*T. ohioensis*	2C-2a
		S. gracilis lower	Cherryvale			2C-1c
	M3	*S. confragus*	Dennis	*S. confragus* *S. cancellosus*	*T. nebraskensis* *T. celebroides*	2C-1a
MC-1	M2	*S. cancellosus*	Swope			1S-4a
	M1	Barrick *I.* n sp A	Hertha			1S-3a
		I. sulciferous	Exline			1S-2a
DS-5	D8	*I. nodocarinatus*	Lost Branch		*Neoganides* ?*Eoschistoceras* pseudozygopleurid gastropod *Idiognathodus expansus*	1S-1a

NOTE: This chart shows all Midcontinent major cyclothems and all Beeman Fm biostratigraphy, but does not show all intermediate and minor sequences for which no biostratigraphy exists and for which correlations are based on lithostratigraphic criteria.

vertical contact with restricted marine deposits or exposure surfaces. The rapidity of the change in depositional environment from exposure to sub-pycnocline to exposure records the high-frequency sea-level oscillations that led to the non-Waltherian conditions.

REGIONAL CORRELATION TO THE MIDCONTINENT: EUSTASY VS. TECTONICS VS. CLIMATE CONTROLS ON SEDIMENTATION

Regional correlation of the Beeman Formation to the Midcontinent through biostratigraphy allows the largely eustatic sea-level curve of the Midcontinent (Heckel, 1986) to be compared to the relative sea-level curve of the Sacramento Mountains and eustatic vs. tectonic vs. climatic controls on deposition to be quantified (Fig. 14, Table 2).

High-amplitude, high-frequency glacio-eustatic sea-level changes are interpreted to have acted throughout Beeman Formation deposition, with absolute sea-level changes ranging from 70 m to 170 m in amplitude (Heckel, 1977; Ross and Ross, 1987) within Milankovitch orbital parameter time bands (approximately 250–500 ka; Heckel, 1986; Figs. 14 and 15). These sea-level oscilla-

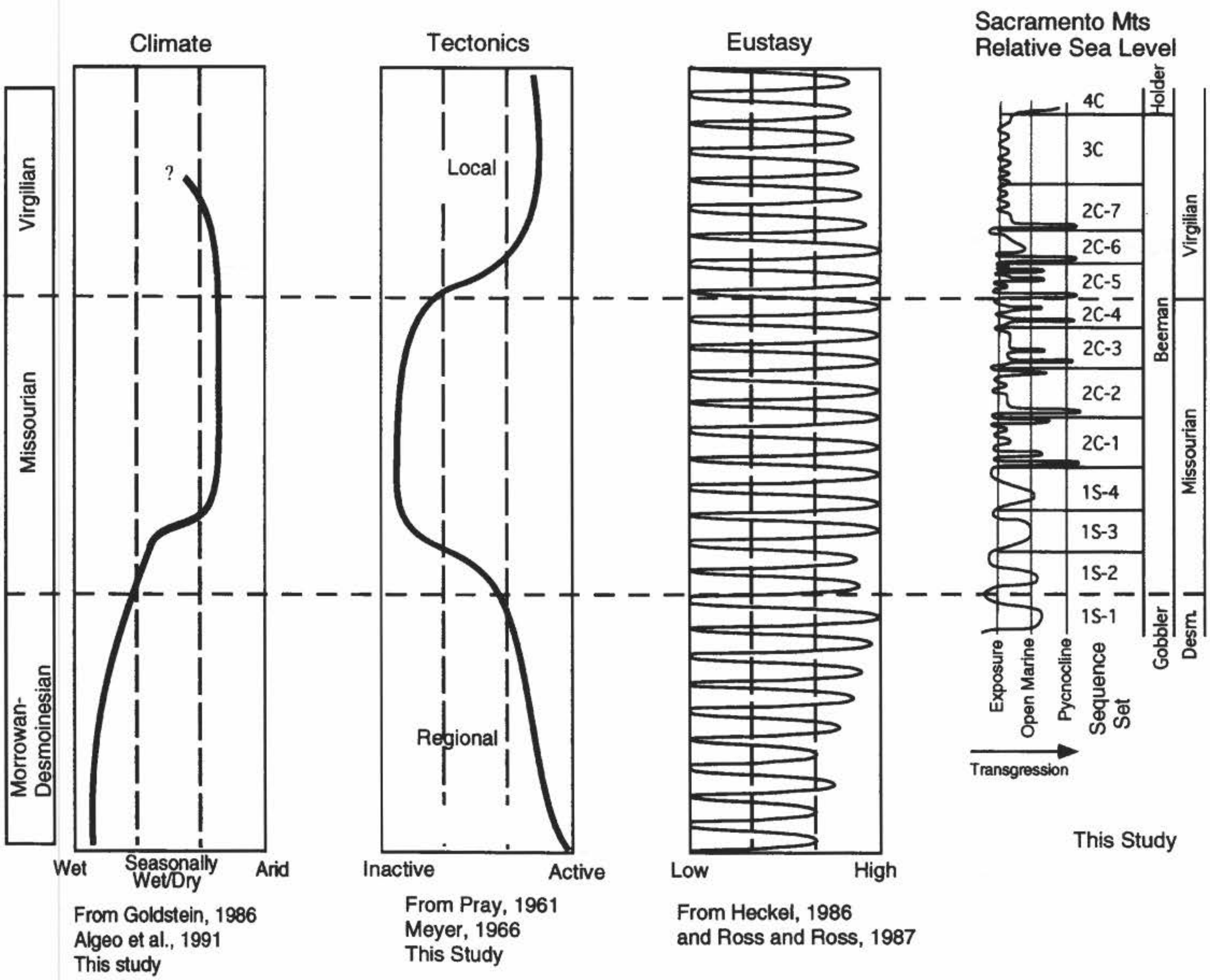

FIGURE 15. Curves of the three major controls affecting Beeman Formation deposition, and the resulting relative curve from the Dry Canyon #2 core.

TABLE 3. Summary of climatic-sensitive variables for Pennsylvanian lithologies in the Sacramento Mountains.

Unit / Description	Desmoinesian	Missourian	Virgilian
	Gobbler Fm	Beeman Fm	Holder Fm
Interpreted paleolatitude	0° to 5° N	5° to 10° N	5° to 10° N
General lithologies	Fluvio-deltaic clatics, Massive carbonates	Lower= fluvio-deltaic clastics, Upper=carbonates	Carbonates, Fluvial and marine clastics
Exposure features	Organic-rich terrestrial shales and meteoric diagenesis	Lower=organic terrestrial shales Upper=rhizoliths, laminar and nodular caliche, "redbed" oxisols, desiccation cracks, blackened grains, autobrecciation, circumgranular cracks, dissolution, dolomite, and silt	Rhizoliths, caliche, autobrecciation, soil glaebules, cracking, blackened grains, evaporites, *Microcodium*, Isopachus spar
Paleosol types	Histosols	Lower=histosols Upper=aridisols (clacisols), oxisols, histosols	Aridisols (calcisols)
Flora and fauna	Plants, open marine	Lower=plants, open marine Upper=open and restricted marine	Plants, open and restricted marine
Climate	Equatorial, humid, hot, little wind, nonseasonal	Tropical, warm, seasonally dry and humid, westerly tradewinds	Tropical, warm seasonally dry and humid, westerly tradewinds

tions are interpreted to be recorded in the individual sequences within the 2C super sequence set of the Beeman Formation.

In addition to the early Pennsylvanian Appalachian tectonic event that formed the Orogrande Basin, the local late Pennsylvanian-Permian pre-Abo compression (Otte, 1959; Pray, 1961) directly affected uppermost Beeman Formation sedimentation through the creation of local highs. High-energy, restricted deposits such as the 3C super sequence set atop the La Luz anticline record scenarios where the tectonic control of sedimentation overrode the glacio-eustatic signal (Figs. 14 and 15).

Climate affected Beeman Formation deposition at two scales. Globally, high-frequency climate changes, perhaps controlled by Milankovitch orbital forcing, were responsible for the growth and ablation of glaciers and the high-amplitude eustatic sea-level oscillations discussed above (Fig. 15). Regionally, continental drift and a continent-wide drying event (Philips and Peppers, 1984) were responsible for a climate shift in the lower Missourian from a Desmoinesian equatorial wet environment with clastic-dominated deposits and Histosol soil development to a middle-upper Missourian tropical seasonally dry environment with carbonate-dominated deposits and Aridisol/Calcisol soil development (Table 3).

CONCLUSIONS

Examining depositional trends at a variety of scales within a detailed sequence stratigraphic framework allows for the recognition and quantification of the effects of eustasy, tectonics, climate, and basin geometry on Beeman Formation deposits. It is significant that despite the active tectonic setting and a major climate shift, the glacio-eustatic signal remained largely dominant. The ability to recognize and biostratigraphically correlate the eustatic signal regionally through major facies changes, climate zones, and tectonic regimes supports the hypothesis that Pennsylvanian cyclothems may be used as global high-resolution chronostratigraphic units.

ACKNOWLEDGEMENTS

Steve Schutter, James Wilson, and Warren Hohertz provided insights and helpful discussions. Exxon Production Research, with special thanks to John Mitchel, allowed access to the Dry Canyon core material. The University of Wisconsin-Madison, Exxon Production Research, and ARCO International Oil and Gas Co. provided funding for this research.

REFERENCES

Algeo, T. J., Wilson, J. L. and Lohmann, K. C., 1991, Eustatic and tectonic controls on cyclic sediment accumulation patterns in Lower-Middle Pennsylvanian strata of the Orogrande Basin, New Mexico: New Mexico Geological Society, Guidebook 42, p. 203–212.

Bachtel, S. L., Rankey, E. C. and Kaufman J., 1997, Sequence stratigraphy of a mixed carbonate-siliciclastic shelf, Holder Formation (Pennsylvanian, Virgilian), Sacramento Mountains, New Mexico: American Association of Petroleum Geologists, Abstracts with Program, v. 6, p. 6.

Bergeron, T. J., 1957, Stratigraphy of the Beeman Formation in Dry Canyon, Alamogordo, New Mexico [M.S. thesis]: Madison, University of Wisconsin, 57 p.

Boardman, D. R. I. and Heckel, P. H., 1989, Glacial-eustatic sea-level curve for early Late Pennsylvanian sequence in north-central Texas and biostratigraphic correlation with curve for Midcontinent: Geology, v. 17, p. 802–805.

Cline, L. M., 1959, Preliminary studies of the cyclical sedimentation and paleontology of the upper Virgil strata of the La Luz area, Sacramento Mountains, New Mexico: Society of Economic Paleontologists and Mineralogists, Permian Basin Section and Roswell Geological Society Guidebook, p. 172–185.

Goldstein, R. H., 1986, Integrative carbonate diagenesis studies: Fluid inclusions in calcium carbonate cement; Paleosols and cement stratigraphy of Late Pennsylvanian cyclic strata, New Mexico [Ph.D. dissertation]: Madison, University of Wisconsin, 361 p.

Goldstein, R. H., 1988, Paleosols of Late Pennsylvanian cyclic strata, New Mexico: Sedimentology, v. 35, p. 777–803.

Heckel, P. H., 1977, Origin of phosphatic black-shale facies in Pennsylvanian cyclotherms of midcontinent North America: American Association of Petroleum Geologists Bulletin, v. 61, p. 1045–1068.

Heckel, P. H., 1986, Sea-level curve for Pennsylvanian eustatic marine transgression-regression depositional cycles along Midcontinent outcrop belt, North America: Geology, v. 14, p. 330–334.

King, P. B., 1942, Permian of west Texas and southeast New Mexico: American Association of Petroleum Geologists Bulletin, v. 26, p. 535–763.

Kluth, C. F. and Coney, P. J., 1981, Plate tectonics of the ancestral Rocky Mountains: Geology, v. 9, p. 10–15.

Kottlowski, F. E., Flower, R. H., Thompson, M. L. and Foster, R. W., 1956, Stratigraphic studies of the San Andres Mountains, New Mexico: New Mexico Bureau of Mines and Mineral Resources, Memoir 1, 132 p.

Meyer, R. F., 1966, Geology of the Pennsylvanian and Wolfcampian rocks in southeast New Mexico: New Mexico Bureau of Mines and Mineral Resources, Memoir 17, 123 p.

Otte, C., 1959, Late Pennsylvanian and early Permian stratigraphy of the northern Sacramento Mountains, Otero County, New Mexico: New Mexico Bureau of Mines and Mineral Resources, Bulletin 50, 111 p.

Phillips, T. L. and Peppers, R. A., 1984, Changing patterns of Pennsylvanian coal-swamp vegetation and implications of climatic control on coal occurrence: International Journal of Coal Geology, v. 3, p. 205–255.

Pray, L. C., 1952, Stratigraphy of the Escarpment of the Sacramento Mountains, Otero County, New Mexico: [Ph.D. dissertation]: California Institute of Technology, 370 p.

Pray, L. C., 1961, Geology of the Sacramento Mountain escarpment, Otero County, New Mexico: New Mexico Bureau of Mines and Mineral Resources, Bulletin 35, 144 p.

Raatz, W. D., Schutter, S. R. and Wilson, J. L., 1994, Missourian strata of the northern Sacramento Mountains and Orogrande Basin, New Mexico; *in* Garber, R. A. and Keller, D. R., eds., Field guide to the Paleozoic section of the San Andres Mountains: Society of Economic Paleontologists and Minerologists, Permian Basin Section, Guidebook 94-35, p. 61–69.

Raatz, W. D. and Simo, J. A., 1995, Eustasy, tectonics and climate: Isolation of controls on Pennsylvanian (Missourian) cyclothems from the Sacramento Mountains (Orogrande Basin) New Mexico: American Association of Petroleum Geologists, Abstracts with Programs, v. 4, p. 79.

Raatz, W. D., 1996, Sequence stratigraphy of the Beeman Formation: Interaction of eustasy, tectonics, and climate on a mixed terrigenous clastic/carbonate shelf and basin, Upper Pennsylvanian, Sacramento Mountains, New Mexico: [Ph.D. dissertation], Madison, University of Wisconsin, 404 p.

Ross, C. A. and Ross, J. R. P., 1987, Late Paleozoic sea levels and depositional sequences; *in* Ross, C. A. and Haman, D., eds., Timing and depositional history of eustatic sequences: Constraints on seismic stratigraphy: Cushman Foundation for Foraminiferal Research, Special Publication 24, p. 137–149.

Schutter, S. R., 1989, Lithologies and depositional environments of the cyclic Beeman Formation (Missourian; Sacramento Mountains, southeastern New Mexico) compared to Midcontinent cyclotherms: Geological Society of America, Abstracts with Programs, v. 21, no. 1, p. 40.

Soreghan, G. S., 1992, Sedimentology and process stratigraphy of the Upper Pennsylvanian Pedregosa (Arizona) and Orogrande (New Mexico) basins [Ph.D. dissertation]: Tucson, University of Arizona, 278 p.

Van Wagoner, J. C., 1977, Lower and middle Pennsylvanian rocks of the northern Sacramento Mountains: A study of contemperaneous carbonate and siliciclastic deposition in an active tectonic setting [Ph.D. dissertation]: Houston, Texas, Rice University, 179 p.

Van Wagoner, J. C., Mitchum, R. M., Campion, K. M. and Rahmanian, V. D., 1990, Siliciclastic sequence stratigraphy in well logs, cores, and outcrops: Concepts for high-resolution correlation of time and facies: American Association of Petroleum Geologists, Methods in Exploration Series, no. 7, 55 p.

Wilson, J. L., 1967, Cyclic and reciprocal sedimentation in Virgilian strata of southern New Mexico: Geological Society of America Bulletin, v. 78, p. 805–818.

Wilson, J. L., 1972, Influence of local structure on sedimentary cycles of Late Pennsylvanian beds of the Sacramento Mountains, Otero County, New Mexico; *in* Elam, J. G. and Chuber, S., eds., Cyclic sedimentation of the Permian Basin, 2nd ed., West Texas Geological Society, p. 100–114.